Gao *et al. Chem. Biol. Technol. Agric.* (2023) 10:31
https://doi.org/10.1186/s40538-023-00404-9

Chemical and Biological Technologies in Agriculture

RESEARCH

Open Access

Effect of nano-calcium carbonate on morphology, antioxidant enzyme activity and photosynthetic parameters of wheat (*Triticum aestivum* L.) seedlings

Yu Gao[1], Shuang Chen[1], Yajun Li[1] and Yan Shi[1*]

Abstract

To meet the human demand for crop productivity, there are several challenges that researchers are involved in the photosynthetic efficiency of plants may be one of them. Nanotechnology can improve agricultural productivity by affecting the photosynthetic activity of plants. However, no studies have yet shown that nano-calcium carbonate (NCC) can play a role in improving photosynthetic performance of plants. In order to explore the effects of NCC on wheat seedling morphology, antioxidant enzyme activities and photosynthetic parameters, wheat roots were exposed to different concentrations of NCC (0, 25, 50, 100, 200, 400 mg L^{-1}) through hydroponic experiments. Different concentrations affected root length, root surface area, root diameter, root volume and plant dry biomass. Compared to the control (0 mg L^{-1} of NCC) application (CK), wheat with 200 mg L^{-1} of NCC application showed 54% and 58% increase in superoxide dismutase (SOD) and ascorbate peroxidase (APX) activities, respectively. As for photosynthesis-related physiological indicators, compared with CK, 200 mg L^{-1} of NCC significantly enhanced chlorophyll a (38%), chlorophyll b (20%), carotenoid content (19%), Rubisco activity (3.02-fold), net photosynthetic rate (Pn, 56%), transpiration rate (Tr, 40%), and stomatal conductance (Gs, 71%). The PCR results showed that compared with CK, the *psbA* gene encoding the photosystem PSII reaction center D1 protein and the *rbcL* gene encoding the large subunit of Rubisco were up-regulated by 2.56- and 2.58-fold at 200 mg L^{-1} NCC treatment, and by 3.22- and 3.57-fold at 400 mg L^{-1} NCC treatment, respectively. Specifically, NCC has significant benefits on wheat seedling growth, and 200 mg L^{-1} is the optimal concentration. NCC enhanced photosynthetic performance of wheat by increasing antioxidant enzyme activity, photosynthetic pigment content, Rubisco activity, stomatal conductance and PSII reaction center activity.

Keywords Nanoparticles, Concentration, Antioxidant system, Photosystem

*Correspondence:
Yan Shi
yanshi@qau.edu.cn
Full list of author information is available at the end of the article

Graphical Abstract

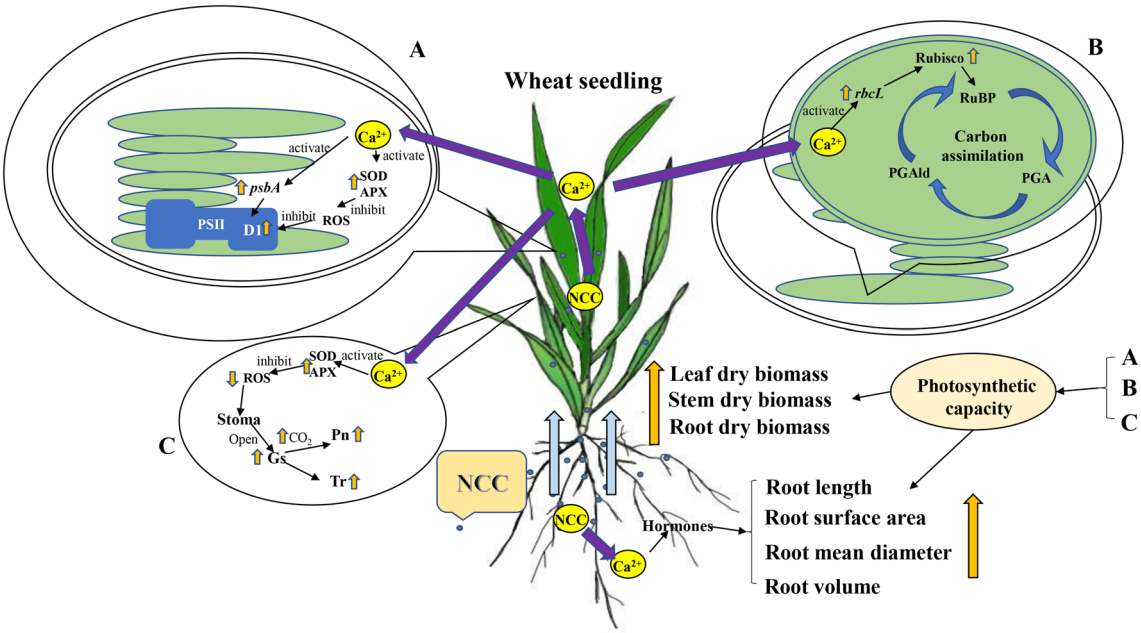

Introduction

As modern agriculture must increase crop productivity to meet the challenges of climate change, declining arable land, and continued population growth, extremely efficient agriculture needs to be developed while reducing global poverty and hunger to meet the high demand for food expected by 2050 [1–3].

Photosynthesis plays an important role in plant growth and development. To meet the rapidly growing human demand for food, energy and materials, there is an urgent need for researchers to find suitable methods to increase the efficiency of plant photosynthesis [4]. Improving crop yields through sustainable approaches such as optimizing the way plants use light are paramount to achieving the sustainable yield growth needed to meet future food demand [5, 6].

Nanoparticles (NPs) are widely used in agriculture to improve the productivity of crops by improving seed germination, seedling growth, photosynthesis, etc. [7, 8]. NPs have been demonstrated to be a novel, powerful and prospective tool for enhancing plant photosynthesis that may revolutionize agriculture in the future, but are currently underutilized [5, 9, 10]. NPs can potentiate photosynthesis in plants by regulating photophosphorylation, carbon assimilation pathway [11], electron transport chain [12], Gs, intercellular CO_2 concentration (Ci), Tr [13], photosynthetic pigment content (chlorophyll a, b, carotenoids) [14], Rubisco carboxylation level [15], etc. The effect of NPs on plant photosynthesis mainly varies depending on the particle size, applied dose, exposure time, surface charge, physicochemical properties of NPs, as well as plant species, growth stage, and cell wall pore size [16–19]. Thus, NPs show both favorable and negative aspects in their effects on plant photosynthesis. Some NPs can inhibit photosynthesis by producing large amounts of reactive oxygen species, reducing chlorophyll content, altering Rubisco activity, and disrupting the building blocks of PSI and PSII [20–23]. NCC has excellent biocompatibility and low toxicity [24, 25] and has minimal poisonous effects on plant photosynthesis. Some investigations have indicated that NCC can promote plant growth by resisting stress [26, 27], but no studies have yet shown that it can play a role in photosynthesis in plants. It is well known that calcium is one of the essential nutrients required for plant growth. In addition to its role in promoting plant growth and development, facilitating plant cell wall construction, and resisting environmental stress [27], it also plays an instrumental role in the photosynthetic pathway [28]. Calcium not only regulates the transcription and translation of genes encoding chloroplast proteins and related enzymes [29], but also participates directly in PSII electron transport [30]. Compared with ordinary calcium carbonate particles, NCC is more

easily absorbed by plants due to its smaller particle size and stronger adhesion [26]. Therefore, the application of NCC may be an effective means to improve photosynthetic efficiency in crops.

To investigate the effects of NCC on photosynthesis and growth and development of wheat seedlings, this study examined the changes in root morphology, aboveground and root biomass, malondialdehyde (MDA) content, antioxidant enzyme activity, photosynthetic pigment content, Rubisco activity, Pn, Tr, Gs, and Ci under different applied doses of NCC by hydroponic experiments. The changes in the expression of *psbA* gene, which encodes the D1 protein of photosystem PSII reaction center, and *rbcL* gene, which encodes the large subunit of Rubisco, were examined by fluorescence quantitative PCR.

Materials and methods

Plants and NCC

Uniform seeds of winter wheat cultivar Taimai 198 were used as the experimental materials in this study. NCC was purchased from Deke Daojin Science and Technology Co., Ltd. (Beijing, China), with a specific surface area of 45–60 m^2 g^{-1} and purity of > 99%. The NCC was characterized using transmission electron microscopy (TEM, Hitachi Ltd., Japan), energy dispersive spectrometer (EDS, Oxford Instrument Co., Ltd., UK), fourier transform infrared spectrometer (FT-IR, Thermo Fisher Scientific, USA) and X-ray diffractometer (XRD, Bruker Technology Co., Ltd.) (Fig. 1).

Characterization of nanoparticle

The shape of the NCC was spherical, and the size of the NCC was determined from the TEM (Fig. 1A), while the XRD pattern was recorded using Cu kα radiation ($\lambda = 0.15406$ nm) at room temperature in the range of $2\theta = 10°–90°$ with a scanning speed of 4° min^{-1}. Ten peaks ($2\theta = 23.08°$, 29.44°, 39.46°, 36.02°, 43.22°, 47.57°, 57.48°, 64.76°, and 60.92°) were selected using Origin2022 software (OriginLab, USA) and calculated the particle size of NCC using Scherrer's formula [31] (Fig. 1D). The final particle size of NCC was obtained as 14–56 nm. Based on the energy spectrum analysis, the specific gravity of Ca was 35.95%, O was 46.85%, C was 17%,

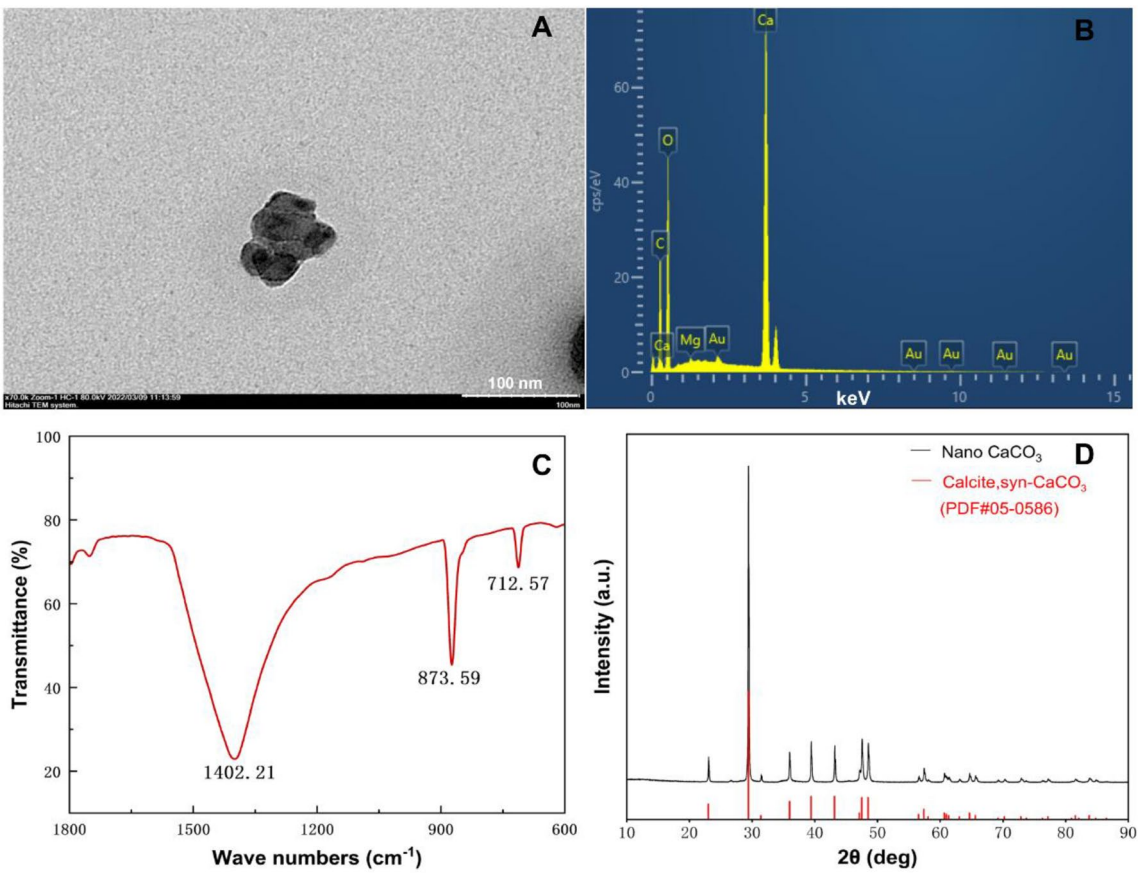

Fig. 1 TEM (**A**), TEM (**B**), FT-IR (**C**), and XRD (**D**) picture of nano-calcium carbonate particles

and other elements were negligible, and the main component of the substance could be identified as $CaCO_3$ (Fig. 1B). According to FT-IR analysis (Fig. 1C), the NCC has absorption peaks at wavenumbers of 1402.21, 873.59, and 712.57 cm^{-1}, and these three peaks are characteristic absorption peaks of calcite-type CO_3 [32], so the NCC is calcite-type CO_3. Based on the XRD analysis (Fig. 1D), the NCC was determined to be calcite-type CO_3 by comparing it with the standard card PDF#05-0586 (calcite) in the range of $2\theta = 10°–90°$, which is the same as the FT-IR results.

Experiment design

The wheat seeds were surface disinfected with 2.5% sodium hypochlorite solution for 10 min, rinsed with sterile distilled water, then placed in Petri dishes for germination. After 10 days, the wheat seedlings that grew to the one-leaf stage with uniform growth were selected and transferred to the setting plate and placed on top of a plastic box (32 cm in length, 24 cm in width, and 12 cm in height) filled with 9 L of nutrient solution (half amount of Hoagland nutrient solution) (Additional file 1: Table S1) so that the wheat roots were immersed in the nutrient solution (Fig. 2 and Additional file 1: Figure S1). Use an electric pump to pump air into the water. The greenhouse temperature was set at 22 °C/18 °C (day/night) with a light of 300 μmol m^{-2} s^{-1} and a photoperiod of 12 h. After 10 days, the wheat was divided into six groups at the three-leaf stage and five groups of different concentrations of NCC solution were set up with no NCC as the control, and three replicates were set up for each treatment (Table 1). The NCC was dissolved in nutrient solution and ultrasonically dispersed with an ultrasonic cell crusher for 10 min so that the NCC were uniformly dispersed in the nutrient solution, and its pH was measured with a pH meter (Shanghai Yidian Scientific Instrument Co., Ltd., China). The NCC suspension was stirred with a magnetic stirrer for 20 min every 12 h, and the NCC suspension and nutrient solution were replaced every 3 days. Sampling was carried out after 10 days of NCC treatment, which was 30 days after the germination of wheat seeds.

Measurements

Root system morphology analysis

Five fresh wheat seedlings were selected for each treatment and wheat roots were immediately separated and each wheat plant was measured separately. The wheat roots were carefully cleaned and placed in a transparent tray with a small amount of water

Table 1 Nano-calcium carbonate dosage

Treatments	Nano-calcium carbonate concentration (mg L^{-1})	pH
CK	0	6.78
T1	25	6.94
T2	50	7.07
T3	100	7.17
T4	200	7.25
T5	400	7.34

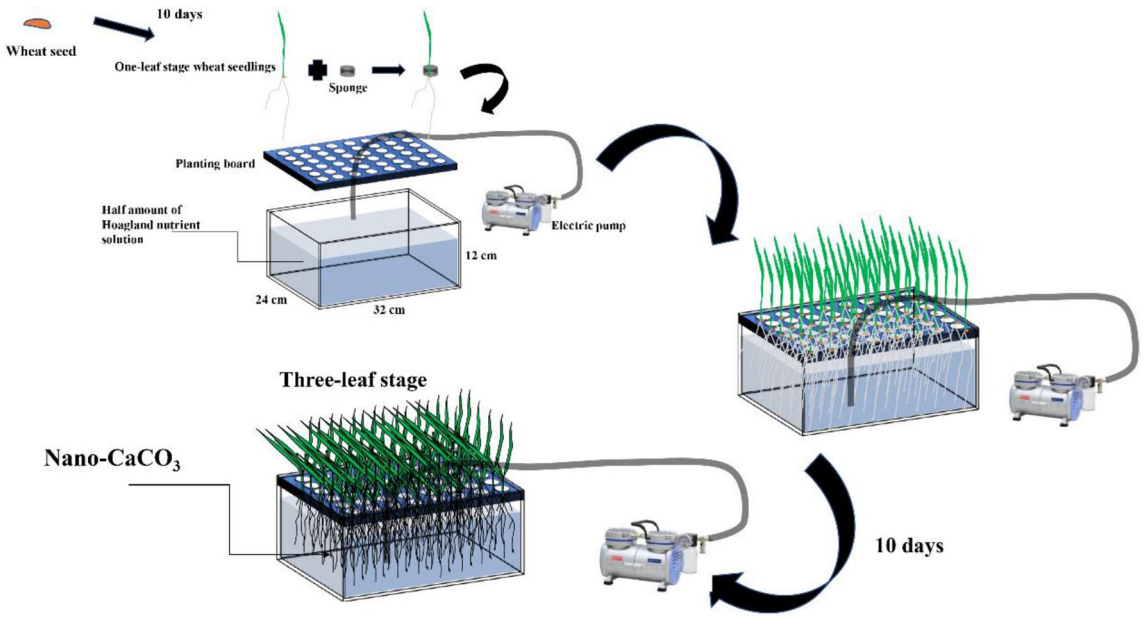

Fig. 2 Schematic diagram of wheat hydroponics

(2–3 mm water layer), and each root of the wheat was separated so that the wheat roots were dispersed in the water. The tray was transferred to LA2400 root scanner (Regent Instruments Inc, Canada). After scanning, root length, root diameter, root surface area, and root volume of wheat were analyzed using WinRHIZO pro software (version 2012b, Regent Instruments Inc., Canada) [14].

Biomass determination

Ten wheat seedlings were taken for each treatment, and the stems, leaves, and roots of wheat seedlings were separated after washing and wiping them clean. They were placed in an oven at 105 °C for 30 min to inactivate the enzyme and then dried at 75 °C to a constant weight [33].

Determination of MDA content and antioxidant enzyme activity

0.5 g of fresh wheat leaves were rapidly frozen in liquid nitrogen and then quickly ground into a homogenate with 5 mL of pre-chilled 4-hydroxyethyl piperazine ethanesulfonic acid (HEPES) buffer (50 mM, pH 7.8) containing 20% (v/v) glycerol, 1 mM disodium ethylenediaminetetraacetate (EDTA Na_2), 1 mM ascorbic acid (AsA), 5 mM $MgCl_2$ and 1 mM dithiothreitol (DTT). The homogenate was transferred to a centrifuge tube and then centrifuged at 10,000*g* for 20 min to obtain the supernatant, which was the enzyme extraction solution.

MDA was determined by the method of [34], 2 mL of enzyme solution was added to 4 mL of trichloroacetic acid–thiobarbituric acid (TCA–TBA) mixture (101.25 g of TCA and 2.5 g of TBA were dissolved by heating, cooled and fixed to 500 mL), boiling water bath for 20 min. After centrifuging at 4000*g* for 10 min, the supernatant was collected and analyzed at 450 nm, 532 nm and 600 nm under a visible spectrophotometer.

SOD activity was determined by photochemical reaction with nitroblue tetrazolium (NBT) [35] with slight modifications. The reaction solution (2.9 mL) was prepared with 50 mmol L^{-1} HEPES buffer (containing 130 mmol L^{-1} methionine, 750 μmol L^{-1} NBT, 100 μmol L^{-1} EDTA Na_2, 60 μmol L^{-1} riboflavin) and 0.1 mL of enzyme extract (pH 7.8). The tubes were exposed to 4000 lx light for 15 min, and the reaction was ended by shading immediately after the light exposure. The absorbance was recorded at 560 nm.

Catalase (CAT) activity was measured by monitoring the decrease in absorbance at 240 nm due to H_2O_2 depletion [36]. APX activity was measured by observing the decrease in absorbance at 290 nm due to the oxidation of ascorbic acid [37].

Determination of chlorophyll and carotenoid contents

Weigh 0.2 g of cut fresh wheat leaves into a pre-cooled mortar, add 3 mL of 80% acetone solution, grind the wheat leaves into a homogenous slurry and then add 10 mL of 80% acetone solution, let it stand for 3–5 min and then filter. The filtrate was transferred to a 25-mL brown reagent bottle, fixed with 80% acetone solution and each treatment was repeated three times. The absorbance was measured by spectrophotometer (Agilent Technologies, USA) at 663 nm, 645 nm, and 470 nm, respectively, using 80% acetone as a blank. The contents of chlorophyll a, chlorophyll b, and carotenoids were calculated according to the formula [38].

Rubisco activity determination

Total Rubisco enzyme of wheat leaves was extracted using Ribulose diphosphate carboxylase kit (Suzhou Kemin Biotechnology Co., Ltd., China). According to the manufacturer's requirements, 0.1 g of fresh wheat leaves were weighed and put into a pre-chilled mortar, then 1 mL of the extract was added to the mortar, and the wheat leaves were ground into a homogenate on ice and transferred to a 2-mL centrifuge tube, and the leaf extract was sonicated with a cell crusher (4 ℃, 200W, 3 s on, 7 s off) for 1 min, then centrifuged at 4 ℃ and 8000*g* for 10 min, and the supernatant was taken for determination.

Rubisco activity was measured by monitoring the decrease in absorbance at 340 nm due to the oxidation of reduced coenzyme I (NADH). 950 μL of reagent provided by the manufacturer and 50 μL of supernatant were added to a quartz cuvette according to the manufacturer's requirements. The absorbance at 340 nm was recorded by spectrophotometer (Agilent Technologies, USA) at 20 s (A1) and 5 min 20 s (A2). Calculations were performed using the following equation:

$$\text{Rubisco (nmol min}^{-1}\text{ g}^{-1}\text{ FW)} = [\Delta A \times V_{RS} \div (\varepsilon \times d) \times 10^9] \div (V_S \div V_T \times W) \div T.$$

Note: ΔA: A1(absorbance value at 20 s) – A2 (absorbance value at 5 min 20 s); V_{RS}: total volume of the reaction system, 1×10^{-3} L; ε: molar extinction coefficient of NADH, 6.22×10^3 (L mol^{-1} cm^{-1}); d: cuvette optical diameter, 1 cm; V_S: volume of added supernatant, 0.05 mL; V_T: volume of added extraction solution, 1 mL; T: reaction time, 5 min; W: sample mass, g.

Determination of Pn, Tr, Gs, and Ci

The Pn, Tr, Gs, and Ci of wheat leaves were measured by a Li-6800 portable photosynthesizer (LI-COR Biosciences, USA) from 9:00 to 11:00 a.m. Three wheat plants were selected for each treatment. The operation of the instrument was based on the experiment of [39], and the parameters were modified. The newly expanded

wheat leaves were placed in a 2 cm^2 leaf chamber with the light quantum flux density set at 800 μmol m^{-2} s^{-1}, the CO_2 concentration maintained at 400 mmol mol^{-1}, the measurement temperature set at 25 °C, the flow rate set at 500 mmol s^{-1}, and the relative air humidity was 65%.

Real-time fluorescence quantitative PCR for gene expression detection

The wheat leaves frozen at − 80 °C were ground into powder form in a mortar pre-cooled with liquid nitrogen, and the mortar was continuously replenished with liquid nitrogen during the grinding process. Total RNA was extracted from 50 to 100 mg of wheat leaf powder using *Steadypure* plant RNA extraction kit (Accurate Biotechnology Co., Ltd, Hunan, China). The purity and concentration of RNA extracts were determined using an Ultramicro ultraviolet visible spectrophotometer (NanoDrop one C, Thermo Fisher Scientific, USA). First-strand cDNA synthesis was performed using *EVO M-MLV* RT Mix Kit (Accurate Biotechnology Co., Ltd, Hunan, China). The SYBR Green premix Pro Taq HS qPCR Kit (Accurate Biotechnology Co., Ltd, Hunan, China) was used according to the manufacturer's instructions on the QuantStudio3 Real-time fluorescence. The relative expression of *psbA* gene encoding photosystem PSII reaction center D1 protein and the gene encoding Rubisco large subunit *rbcL* was calculated by the $2^{-\Delta\Delta Ct}$ method [40] using *Actin* as the reference gene in real-time quantitative PCR on a QuantStudio3 Real-time fluorescence quantitative PCR system (Applied Biosystems, USA). The primers for the relevant genes are shown in Table 2.

Data analysis

SPSS 26.0 (IBM, USA) was used for data analysis. The Shapiro–Wilk test and Levene test were applied to verify the normality of variables and homogeneity of the variance, respectively, followed by one-way ANOVA on the data. Tukey's test ($P<0.05$) was used for post hoc multiple comparisons, and marked letters were used to indicate significant differences between treatments.

Results

Root system morphology

In general, root length, root surface area, root diameter, and root volume of wheat seedlings treated with NCC increased (Table 3, Fig. 2). Root length was significantly greater in the T1, T2, T3, T4, and T5 treatments than in CK, being 39%, 43%, 68%, 81%, and 76% higher than in CK, respectively. Similar results were observed in root surface area and root volume. Compared to CK, root surface area increased by 42%, 50%, 68%, 100%, and 97% and root volume increased by 45%, 47%, 65%, 122%, and 114% for T1, T2, T3, T4, and T5, respectively. While there was no significant difference in root diameter between CK, T1, and T2, root diameter was significantly greater in T3, T4, and T5, increasing by 6%, 18%, and 15%, respectively, compared to CK. There was no significant difference in root length, root surface area, root diameter, and root volume between T4 and T5, but T4 was slightly higher than T5 (Fig. 3).

Table 2 Sequence of gene primers

Primer name	Forward sequence (5′–3′)	Reverse sequence (5′–3′)	References
Actin	GGGACCTCACGGATAATCTAATG	CGTAAGCGAGCTTCTCCTTTAT	[41]
psbA	CAAGGTTAGCACGGTTGATGA	GCTGCTTGGCCTGTAGTAGGA	[42]
rbcL	GATACCGCGAGCACGATCTT	CGCGACAATGGCCTACTTCT	[42]

Table 3 Effects of different concentrations of nano-calcium carbonate on root morphology of wheat seedlings

Treatments	Root length (m)	Root surface area (cm^2)	Root mean diameter (mm)	Root volume (cm^3)
CK	3.97 ± 0.17 c	29.54 ± 1.49 d	0.234 ± 0.006 c	0.18 ± 0.01 c
T1	5.53 ± 0.24 b	41.97 ± 2.19 c	0.242 ± 0.003 bc	0.25 ± 0.02 b
T2	5.67 ± 0.16 b	44.16 ± 5.52 c	0.237 ± 0.005 c	0.26 ± 0.03 b
T3	6.67 ± 0.29 a	49.67 ± 3.24 b	0.248 ± 0.009 b	0.29 ± 0.02 b
T4	7.18 ± 0.61 a	59.02 ± 3.96 a	0.275 ± 0.009 a	0.39 ± 0.04 a
T5	6.97 ± 0.53 a	58.15 ± 6.00 a	0.270 ± 0.005 a	0.37 ± 0.05 a

Different letters in the same column represent significant differences ($p<0.05$). The results were presented as mean ± SD (standard deviation)

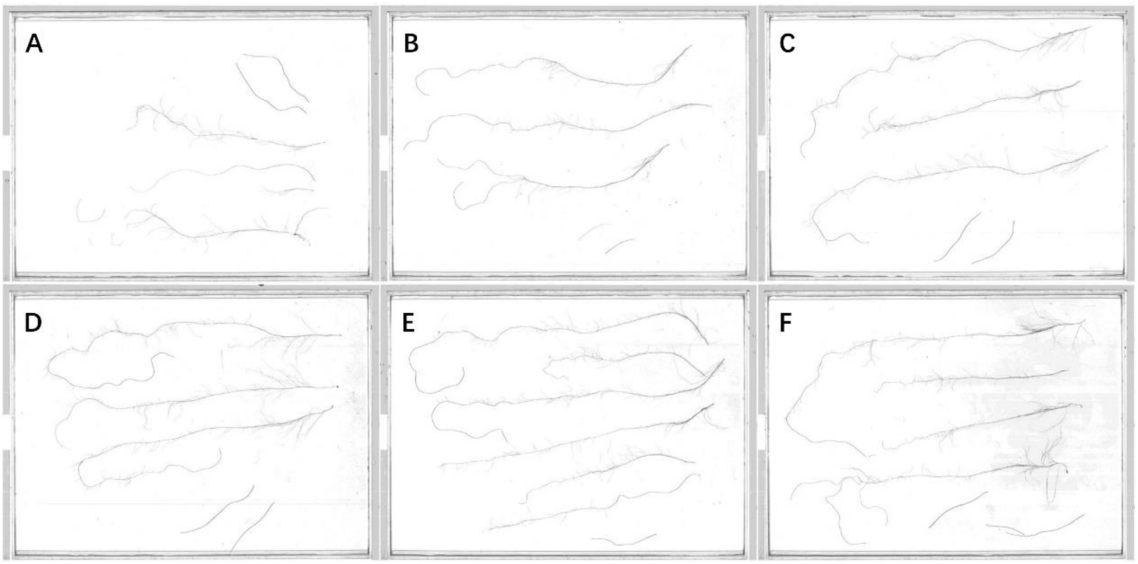

Fig. 3 Effects of different concentration of nano-calcium carbonate on root morphology of wheat seedlings. **A**–**F** Represent the different treatments (CK, T1, T2, T3, T4 and T5), respectively

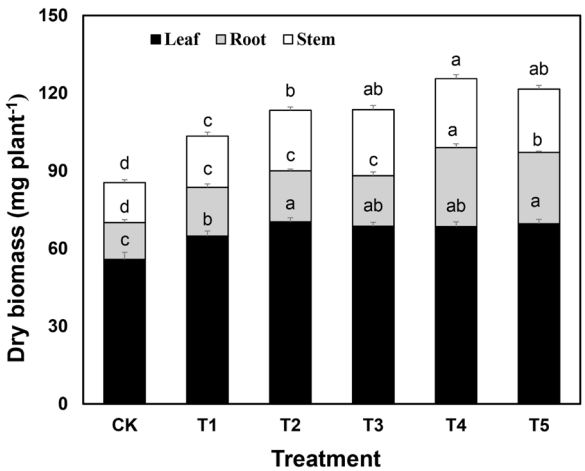

Fig. 4 Effects of different concentrations of nano-calcium carbonate on root, stem and leaf biomass of wheat seedlings. The different letters above the error line represent the significant difference in the mean values of different treatments of the same measurement item ($P < 0.05$)

Biomass

The dry biomass of roots, stems and leaves increased in all wheat seedlings (T1, T2, T3, T4, and T5) treated with NCC (Fig. 4). Root dry weight was significantly higher in T4 compared to the other treatments, increasing by 114%, 62%, 55%, 56% and 10% in T4 compared to CK, T1, T2, T3 and T5. The maximum stem dry biomass was also observed in T4, with a significant increase of 73% compared to CK. While the maximum leaf dry weight appeared in T2, leaf dry biomass in T2, T3, T4 and T5 were not significantly different, but all were significantly greater than CK, increasing by 26%, 23%, 23% and 25%, respectively, compared to CK.

MDA content and antioxidant enzyme activity

As demonstrated in Fig. 5, the SOD and APX activities of wheat seedling leaves were increased after the treatment with NCC. Compared with CK, SOD activity was significantly increased by 27%, 54%, and 49% in T2, T4, and T5, respectively. APX activity was significantly increased by 40%, 32%, 58%, and 51% in T1, T3, T4, and T5, respectively. The differences in CAT activity and MDA content were not significant for all treatments.

Photosynthetic pigments

From Fig. 6, chlorophyll a, chlorophyll b and carotenoid contents of wheat leaves reached their maximum values in T4. The chlorophyll a contents of T1, T2, T3, T4, and T5 were significantly higher than those of CK, with increases of 15%, 15%, 18%, 38%, and 27%, respectively, compared to CK. The chlorophyll b and carotenoid contents of CK, T1, T2, and T3 were not significantly different. The chlorophyll b contents of T4 and T5 treatments were significantly higher than CK by 20% and 13%, and their carotenoid contents were higher than CK by 19% and 12%, respectively.

Rubisco activity

Overall, the Rubisco activity of wheat seedlings treated with different concentrations of NCC increased (Fig. 7). The Rubisco activity of wheat leaves under T4

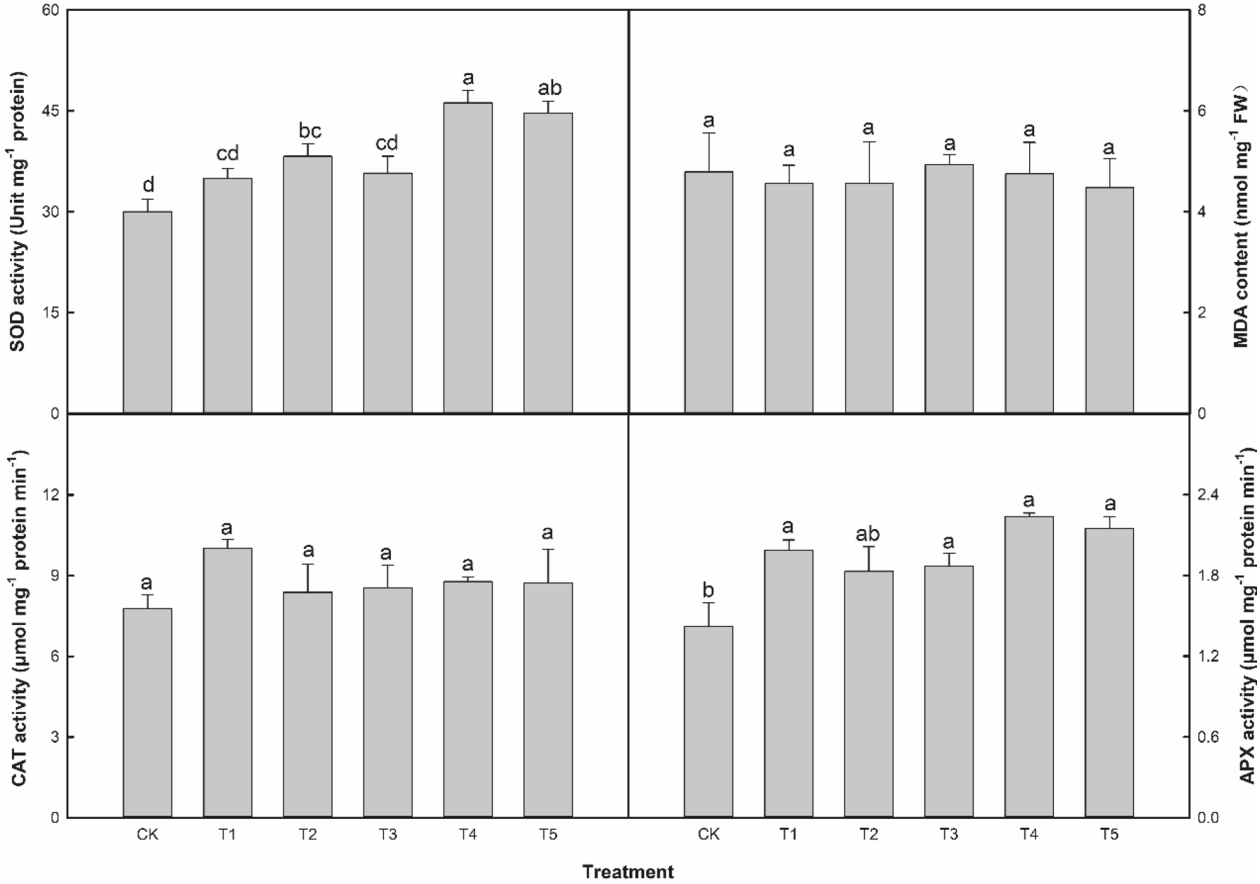

Fig. 5 Effects of different concentrations of nano-calcium carbonate on SOD activity, MDA content, CAT activity, and APX activity in wheat leaves. The different letters above the error line represent the significant difference in the mean values of different treatments of the same measurement item ($P < 0.05$)

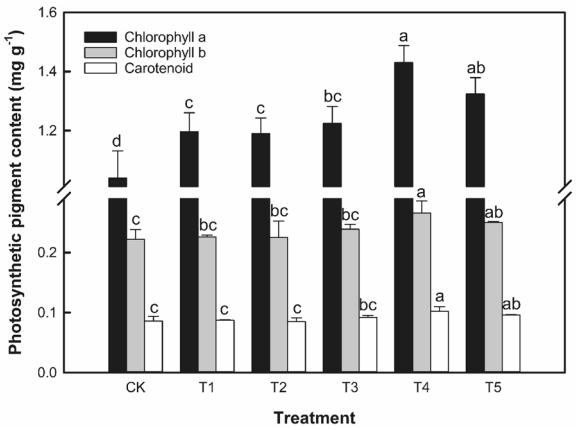

Fig. 6 Effects of different concentrations of nano-calcium carbonate on chlorophyll a, chlorophyll b and carotenoids in wheat leaves. The different letters above the error line represent the significant difference in the mean values of different treatments of the same measurement item ($P < 0.05$)

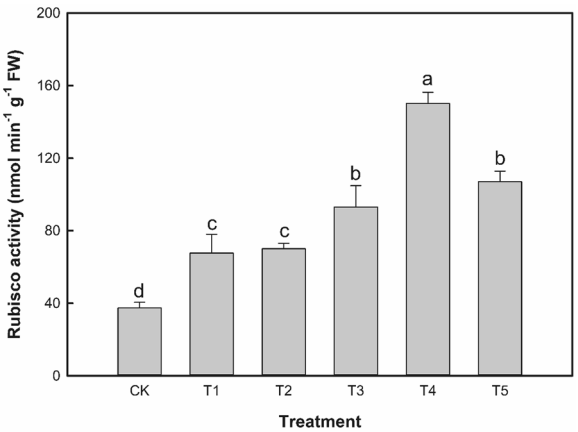

Fig. 7 Effects of different concentrations of nano-calcium carbonate on Rubisco activity in wheat leaves. The different letters above the error line represent the significant difference in the mean values of different treatments of the same measurement item ($P < 0.05$)

treatment was significantly higher than the other treatments. The Rubisco activity of T1, T2, T3, T4, and T5 significantly increased compared to CK by 0.81-, 0.87-, 1.49-, 3.02-, and 1.86-fold.

Relative expression of *psbA* and *rbcL* genes

According to Fig. 8, the expression of *psbA* gene encoding photosystem PSII reaction center D1 protein and *rbcL* gene encoding Rubisco large subunit were up-regulated in wheat seedlings treated with NCC. *psbA* gene expression was 2.56- and 3.22-fold higher in T4 and T5 than in CK, and *rbcL* gene expression was 2.58- and 3.57-fold higher in CK, respectively. The relative expressions of *psbA* and *rbcL* genes were not significantly different in CK, T1, T2 and T3.

Pn, Tr, Gs, and Ci

As indicated in Fig. 9, the Pn, Tr, and Gs of wheat in T4 reached their maximum values and increased by 56%, 40%, and 71%, respectively, compared with CK. The Pn of T1, T2, T3, T4, and T5 were significantly higher than those of CK. The Tr of T4 were significantly higher than those of CK and T1, while the differences in Tr of CK, T1, T2, T3, and T5 were not significant. The Gs of T3 and T4 was significantly higher than that of CK, T1, and T5, while the difference in stomatal conductance of CK, T1, T2, and T5 was not significant. The Ci reached its maximum in CK and was not significantly different in CK, T1, T2, T3, and T5. The Ci in T4 was significantly lower than CK by 8%.

Discussion

Nanometer calcium carbonate activates wheat antioxidant enzyme activity and promotes the germination of wheat seedlings

Calcium is essential for plant growth and development, and it plays an important role in promoting cell metabolism, maintaining cell function, and facilitating plant growth and development [43]. Domingues, Ribeiro, Andriolo, Possobom and Zemolin [44] revealed that calcium concentrations of 2.2 to 4.5 mmol L^{-1} increased dry weight of soybean stems, leaves, and roots. 5 mM calcium carbonate treatment increased aboveground fresh weight, dry weight, root length, and plant height of djulis by 37%, 17%, 55%, and 12%, respectively [45]. Calcium fertilization can promote poplar root growth [46]. Calcium regulates plant root development and growth by interfering with or altering plant hormone levels and regulating the glutamate receptor-like protein AtGLR3.6 [47]. This study showed that NCC increased root length, root surface area, root diameter, root volume, and dry biomass of wheat as a result of direct contact of NCC with the wheat root system. While root length, root surface area, root diameter, root volume and root dry biomass of wheat were slightly reduced in 400 mg L^{-1} NCC concentration treatment compared to those in 200 mg L^{-1} NCC concentration, which could be the result of high concentration of NPs blocking root cells by adhering to them and preventing root adsorption of nutrients [48].

The pH of the nutrient solution increased with the amount of NCC (Table 1), and the correlation between inter-root pH and exogenous organic acids indicated that if a higher inter-root pH could be maintained, the concentration of exogenous organic acids could be increased [49]. Organic acids released from wheat roots promote

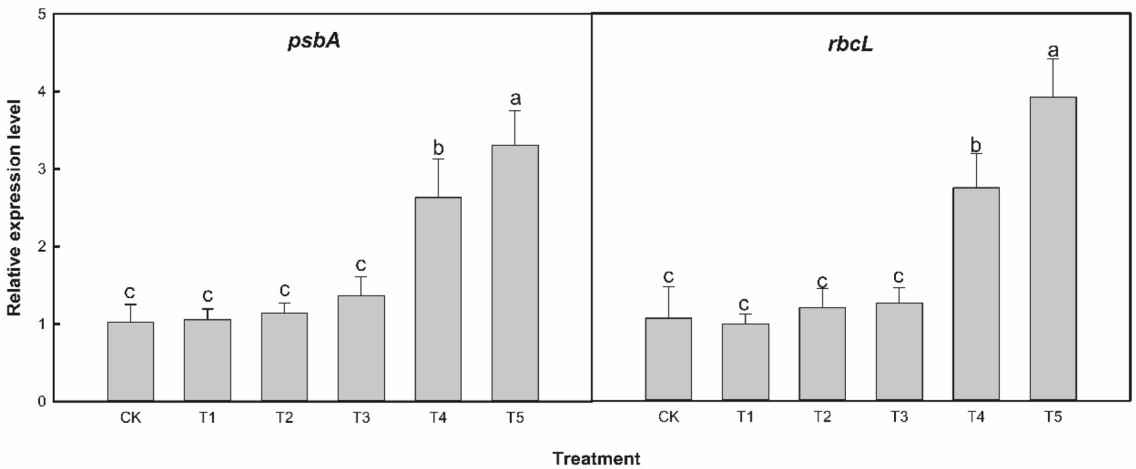

Fig. 8 Effects of different concentrations of nano-calcium carbonate on the relative expression of *psbA* and *rbcL* genes in wheat. The different letters above the error line represent the significant difference in the mean values of different treatments of the same measurement item ($P < 0.05$)

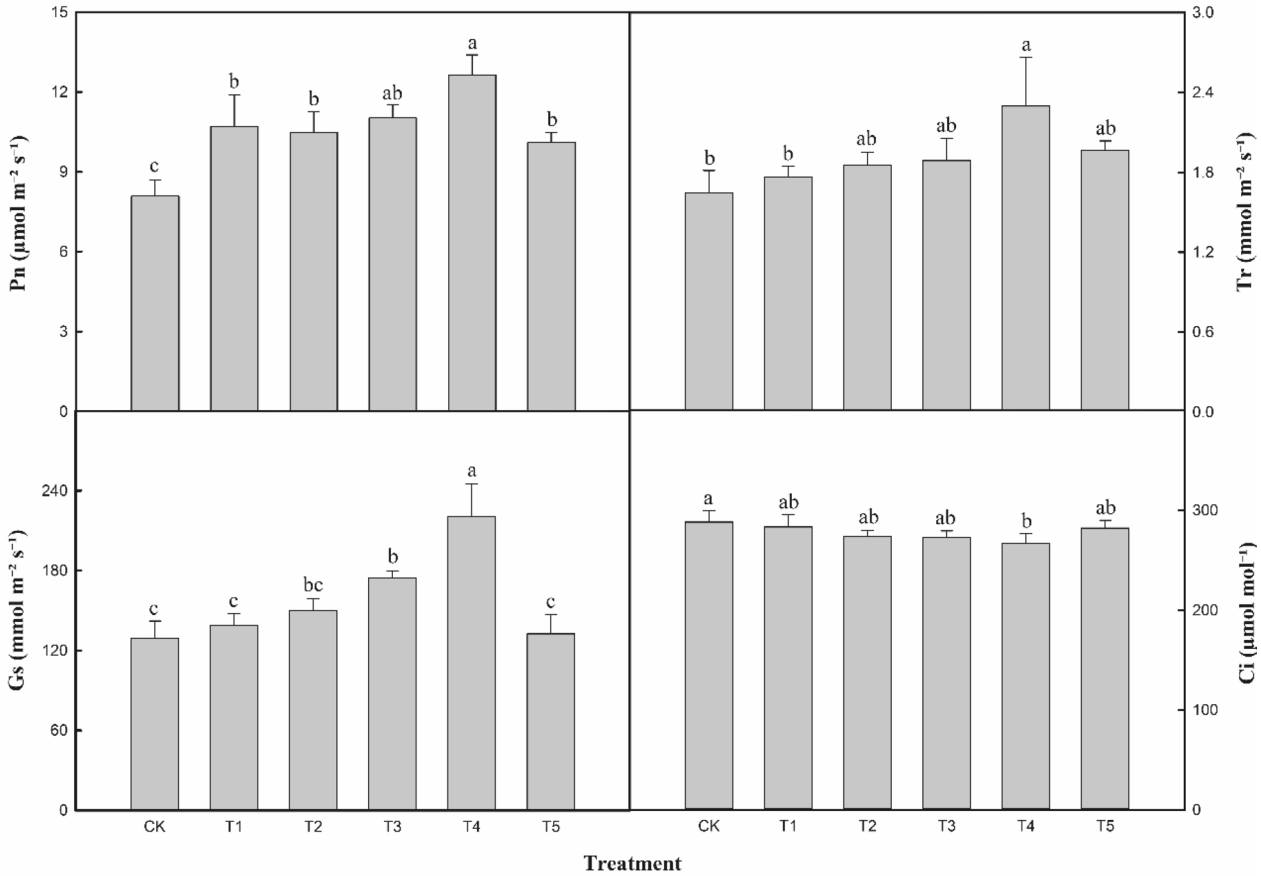

Fig. 9 Effects of different concentrations of nano-calcium carbonate on Pn, Tr, Gs, and Ci in wheat leaves. The different letters above the error line represent the significant difference in the mean values of different treatments of the same measurement item ($P < 0.05$)

the release of Ca^{2+} and increase the uptake of Ca^{2+} by wheat roots. Alternatively, compared with ordinary calcium carbonate, NCC possesses a smaller particle size and larger specific surface area, and has a larger contact area with the wheat root system, making it easier to interact. When exposed to plant roots, NPs can penetrate through root tips, root hairs, lateral roots, root bark and rupture, transfer through the symplastic and apoplastic pathways and finally transfer through xylem and bast and distribute to above-ground parts of the plant, including stems and leaves [9]. However, the uptake and translocation pathways of NCC in plants are poorly understood and may enter through endocytosis [50], carrier proteins [51], intercellular filaments [52], pore-forming behavior [53] or cleavage patterns [54] enter and have an impact on plant life activities.

Plants have enzymatic and nonenzymatic antioxidant systems that can continuously scavenge harmful reactive oxygen species (ROS), but they are exposed to the deleterious effects of abiotic stress when the destructive capacity of abiotic stress is stronger than the capacity of cellular self-defense [55]. Therefore, the accurate spatiotemporal response of defense systems to stress stimuli before the onset of stressful damage is critical for plant survival in response to stressful environmental conditions [55].

An important role of exogenous calcium in activating antioxidant enzyme activity in plants has been demonstrated [56, 57]. A hydroponic study indicated that SOD, CAT, APX and glutathione reductase activities were significantly increased in Taiwan quinoa treated with 5 mM calcium carbonate [45]. NPs play an essential role in protecting plants from various abiotic stresses by stimulating the activity of antioxidant enzymes [58]. Application of nano-mineral analcite promoted CAT activation in maize [59]. Both foliar spray of nano-titanium dioxide and nano-silica reduced electrolyte leakage and malondialdehyde content and increased SOD, POD, CAT and APX activities in rice seedlings [16]. The present study demonstrated that NCC promotes SOD and APX activities in wheat seedlings and plays an important role in scavenging ROS and protecting the photosynthetic system.

This may be because Ca^{2+} acts as a second messenger in response to biotic and abiotic stress signals [60]. The cytoplasmic Ca^{2+} content is regulated by the environment, and adversity activates Ca^{2+} channels, ion pumps or Ca^{2+} transporter proteins embedded in the plasma or organelle membranes to promote Ca^{2+} inward flow [61, 62]. Ca^{2+} and Ca^{2+} transporter proteins are involved in various stress signaling pathways and regulate the activities of antioxidant enzymes such as SOD and APX [62]. In contrast, NCC is more readily absorbed and transported by plants than regular calcium carbonate [26], which means that NCC has a stronger bioavailability. However, to avoid Ca^{2+} toxicity, the cytoplasm was maintained at a low calcium concentration (< 0.1 μM) under resting conditions [63]. Cytoplasmic calcium levels represent the balance between the influx of exogenous Ca^{2+} and the removal of reactive ions from the cytoplasm [64]. To restore cytoplasmic free Ca^{2+} concentration($[Ca^{2+}]$ cyt), active Ca^{2+} transporters (Ca^{2+}/H^{+} exchangers and Ca^{2+} pumps) promote the efflux of excess Ca^{2+} [64]. In contrast, excessive NCC treatment (T5) may produce more Ca^{2+}, which may enter the cytoplasm through passive transport and raise the cytoplasmic Ca^{2+} level, which may damage plant cells when the active Ca^{2+} transporter is not sufficient to restore $[Ca^{2+}]$cyt, which may explain the reduction in some physiological indicators in T5 treatment compared to T4 treatment.

NCC enhances photosynthetic performance of wheat seedlings

Factors affecting the efficiency of photosynthesis include the structural configuration of organelles involved in photosynthesis, structural integrity of chloroplasts and chloroplasts, adequate basal granule development, CO_2 aggregation, Rubisco activity, pigments that aid photosynthesis such as chlorophyll a and chlorophyll b, and the adequate presence of regulatory proteins of thylakoids [65, 66].

Calcium functions in the maintenance of photosynthesis by regulating the expression of chlorophyll synthesis-related genes in leaves [67]. In the present study, we found that NCC also promoted the accumulation of chlorophyll a, chlorophyll b and carotenoids, which reached a maximum at NCC concentration of 200 mg L^{-1}.

NPs may enhance photosynthetic performance mainly by affecting the Hill reaction and Calvin cycle (PSI and PSII activity), leading to greater photophosphorylation [5]. The *psbA* gene encodes the D1 protein, a structurally and functionally important protein at the center of the photosynthetic system II reaction [68]. 200 mg L^{-1} and 400 mg L^{-1} of NCC significantly promoted the up-regulation of *psbA* expression, suggesting that NCC may enhance photosynthetic performance by enhancing D1 protein activity to increase PSII activity. ROS can inhibit D1 protein recombination, while NCC can reduce ROS accumulation by increasing antioxidant enzyme activity [29]. The enhancement of photosynthetic efficiency by NPs may also result from the up-regulation of key photosynthetic enzymes such as Rubisco and Rubisco activating enzyme, etc. [9, 69]. Rubisco is an enzyme that catalyzes ribulose-1,5-bisphosphate carboxylation and oxygenation, the first step in a competing metabolic pathway for carbon dioxide fixation by photorespiration and photosynthesis in higher plants [70]. The results of the experiment showed that Rubisco activity was significantly increased in all treatments with NCC application. *rbcL*, a chloroplast gene encoded by the Rubisco substrate binding center and activity center located in the large subunit, regulates Rubisco synthesis and activity. *rbcL* gene was significantly up-regulated in wheat seedlings cultured in 200 mg L^{-1} and 400 mg L^{-1} of NCC, indicating that NCC can enhance Rubisco activity by strengthening the activity of Rubisco substrate binding center and active center.

The Pn, Tr, and Gs of wheat were significantly increased in NCC treatment. This may be because calcium can affect gas exchange processes associated with photosynthesis by regulating stomatal movement [29]. The earliest sign of stomatal closure is the accumulation of ROS in the outer plastids and chloroplasts, and subsequently, cytoplasmic Ca^{2+} levels control the activity of various kinases, which in turn regulate the activity of ROS-generating enzymes and the activity of various ion channels and in this way regulate stomatal opening and closing [71]. The presence of amylase in guard cells can regulate water content and thus stomatal movement through soluble sugars produced by starch degradation [72]. The accumulation of H_2O_2 can inhibit amylase activity, reduce soluble sugar content, and inhibit stomatal opening [29]. NCC increased enzyme activities such as SOD and APX, reduced the content of ROS and H_2O_2 in guard cells, opened stomata, increased stomatal conductance of wheat leaves, and further increased net photosynthetic rate and transpiration rate. Meanwhile, the accumulation of chlorophyll content and the enhancement of Rubisco activity promoted the fixation of CO_2 and improved photosynthetic performance (Fig. 10).

Conclusion

The effects of different concentrations of NCC on the germination of wheat seedlings were determined by measuring the antioxidant enzyme activity and photosynthetic characteristics of wheat seedlings. 200 mg L^{-1} of NCC was the optimum concentration for germination of wheat seedlings. (1) NCC enhances D1 protein activity by increasing antioxidant enzyme activity and promoting *psbA* expression; (2) NCC promotes

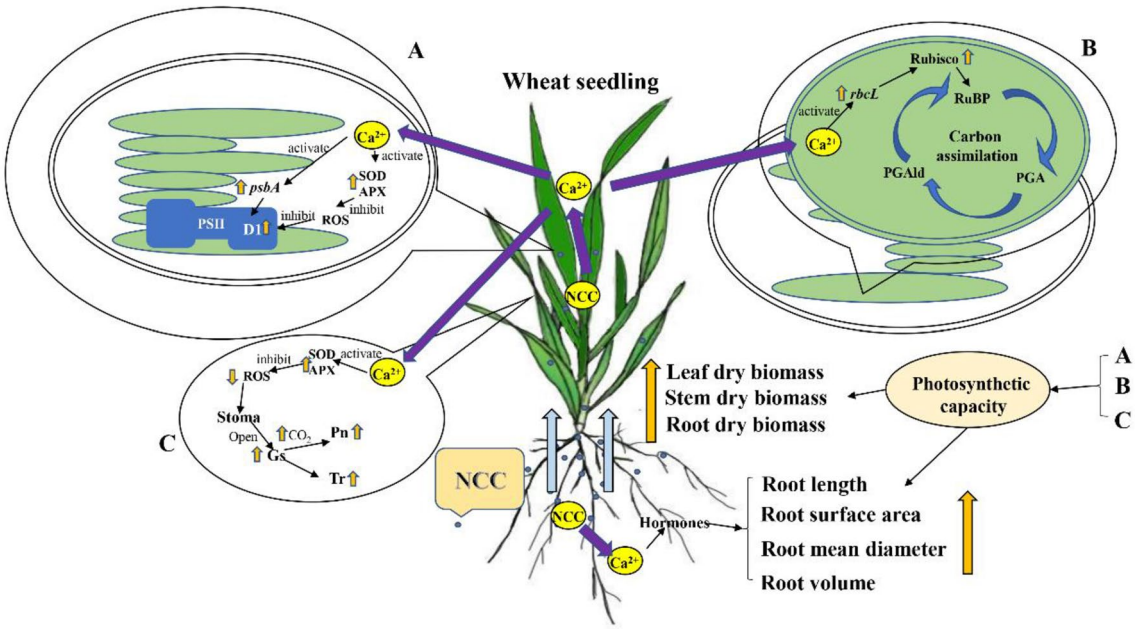

Fig. 10 Mechanism of nano-calcium carbonate to promote the growth of wheat seedlings. RuBP: ribulose-1,5-bisphosphate; PGA: 3-phosphoglycerate; PGAld: 3-phosphoglyceraldehyde

photosynthetic carbon assimilation by increasing Rubisco activity by promoting *rbcL* expression; (3) NCC promotes wheat seedling growth by increasing Gs, Pn, and Tr by increasing antioxidant enzyme activity.

Supplementary Information

The online version contains supplementary material available at https://doi.org/10.1186/s40538-023-00404-9.

Additional file 1. Table S1. Hogland nutrient solution formula. **Figure S1.** Photos of wheat hydroponics system.

Author contributions

YG and YS designed the experiment. YG, SC and YL completed the experiment. YG carried out data analysis and graphic production. YG participated in the writing of manuscript. YG and YS performed the final editing of the manuscript. All authors read and approved the final manuscript.

Funding

Supported by Shandong Modern Agricultural Technology & Industry System—cultivation and soil fertilizer (SDAIT0107) and Agricultural Major Technology Collaborative Promotion Plan Project in Shandong Province (SDNYXTTG-2022-18).

Availability of data and materials

The datasets used or analyzed during the current study are available from the corresponding author on reasonable request.

Declarations

Ethics approval and consent to participate

Meets ethical standards applicable to the research discipline.

Consent for publication

All authors agree to the publication of the work.

Competing interests

The authors declare that there is no conflict of interest.

Author details

[1]Dryland-Technology Key Laboratory of Shandong Province, College of Agronomy, Qingdao Agricultural University, Qingdao, China.

Received: 4 February 2023 Accepted: 6 April 2023
Published online: 19 April 2023

References

1. Folberth C, Skalsky R, Moltchanova E, Balkovic J, Azevedo LB, Obersteiner M, van der Velde M. Uncertainty in soil data can outweigh climate impact signals in global crop yield simulations. Nat Commun. 2016;7:11872. https://doi.org/10.1038/ncomms11872.
2. Ray DK, Gerber JS, MacDonald GK, West PC. Climate variation explains a third of global crop yield variability. Nat Commun. 2015;6:5989. https://doi.org/10.1038/ncomms6989.
3. Zhang X, Davidson EA, Mauzerall DL, Searchinger TD, Dumas P, Shen Y. Managing nitrogen for sustainable development. Nature. 2015;528:51–9. https://doi.org/10.1038/nature15743.
4. Vass I, Cser K, Cheregi O. Molecular mechanisms of light stress of photosynthesis. Ann N Y Acad Sci. 2007;1113:114–22. https://doi.org/10.1196/annals.1391.017.
5. Swift TA, Oliver TAA, Galan MC, Whitney HM. Functional nanomaterials to augment photosynthesis: evidence and considerations for their responsible use in agricultural applications. Interface Focus. 2019;9:20180048. https://doi.org/10.1098/rsfs.2018.0048.
6. Foyer CH, Ruban AV, Nixon PJ. Photosynthesis solutions to enhance productivity. Philos Trans R Soc Biol Sci. 2017;372:20160374. https://doi.org/10.1098/rstb.2016.0374.
7. Das S, Debnath N, Pradhan S, Goswami A. Enhancement of photon absorption in the light-harvesting complex of isolated chloroplast in the presence of plasmonic gold nanosol—a nanobionic approach towards photosynthesis and plant primary growth augmentation. Gold Bulletin. 2017;50:247–57. https://doi.org/10.1007/s13404-017-0214-z.

8. Zulfiqar F, Navarro M, Ashraf M, Akram NA, Munne-Bosch S. Nanofertilizer use for sustainable agriculture: advantages and limitations. Plant Sci. 2019. https://doi.org/10.1016/j.plantsci.2019.110270.
9. Ghorbanpour M, Movahedi A, Hatami M, Kariman K, Bovand F, Shahid MA. Insights into nanoparticle-induced changes in plant photosynthesis. Photosynthetica. 2021;59:570–86. https://doi.org/10.32615/ps.2021.049.
10. Djanaguiraman M, Nair R, Giraldo JP, Prasad PVV. Cerium oxide nanoparticles decrease drought-induced oxidative damage in sorghum leading to higher photosynthesis and grain yield. ACS Omega. 2018;3:14406–16. https://doi.org/10.1021/acsomega.8b01894.
11. Pradhan S, Patra P, Mitra S, Dey KK, Basu S, Chandra S, Palit P, Goswami A. Copper nanoparticle (CuNP) nanochain arrays with a reduced toxicity response: a biophysical and biochemical outlook on vigna radiata. J Agric Food Chem. 2015;63:2606–17. https://doi.org/10.1021/jf504614w.
12. Giraldo JP, Landry MP, Faltermeier SM, McNicholas TP, Iverson NM, Boghossian AA, Reuel NF, Hilmer AJ, Sen F, Brew JA, Strano MS. Plant nanobionics approach to augment photosynthesis and biochemical sensing. Nat Mater. 2014;13:400–8. https://doi.org/10.1038/nmat3890.
13. Gao J, Xu G, Qian H, Liu P, Zhao P, Hu Y. Effects of nano-TiO2 on photosynthetic characteristics of *Ulmus elongata* seedlings. Environ Pollut. 2013;176:63–70. https://doi.org/10.1016/j.envpol.2013.01.027.
14. Hussain S, Iqbal N, Brestic M, Raza MA, Pang T, Langham DR, Safdar ME, Ahmed S, Wen B, Gao Y, Liu W, Yang W. Changes in morphology, chlorophyll fluorescence performance and Rubisco activity of soybean in response to foliar application of ionic titanium under normal light and shade environment. Sci Total Environ. 2019;658:626–37. https://doi.org/10.1016/j.scitotenv.2018.12.182.
15. Linglan M, Chao L, Chunxiang Q, Sitao Y, Jie L, Fengqing G, Fashui H. Rubisco Activase mRNA expression in spinach: modulation by nanoanatase treatment. Biol Trace Elem Res. 2008;122:168–78. https://doi.org/10.1007/s12011-007-8069-4.
16. Rizwan M, Ali S. Effect of foliar applications of silicon and titanium dioxide nanoparticles on growth, oxidative stress, and cadmium accumulation by rice (Oryza sativa). Acta Physiol Plant. 2019;41:35. https://doi.org/10.1007/s11738-019-2828-7.
17. Verma SK, Das AK, Gantait S, Kumar V, Gurel E. Applications of carbon nanomaterials in the plant system: A perspective view on the pros and cons. Sci Total Environ. 2019;667:485–99. https://doi.org/10.1016/j.scitotenv.2019.02.409.
18. Pagano L, Maestri E, Caldara M, White JC, Marmiroli N, Marmiroli M. Engineered Nanomaterial Activity at the Organelle Level: Impacts on the Chloroplasts and Mitochondria. ACS Sustainable Chemistry & Engineering. 2018;6:12562–79. https://doi.org/10.1021/acssuschemeng.8b02046.
19. Tighe-Neira R, Carmora E, Recio G, Nunes-Nesi A, Reyes-Diaz M, Alberdi M, Rengel Z, Inostroza-Blancheteau C. Metallic nanoparticles influence the structure and function of the photosynthetic apparatus in plants. Plant Physiol Biochem. 2018;130:408–17. https://doi.org/10.1016/j.plaphy.2018.07.024.
20. Kataria S, Jain M, Rastogi A, Živčák M, Brestic M, Liu S and Tripathi DK (2019) Chapter 6 - Role of Nanoparticles on Photosynthesis: Avenues and Applications. In: Tripathi DK, Ahmad P, Sharma S, Chauhan DK and Dubey NK (eds) Nanomaterials in Plants, Algae and Microorganisms Academic Press, pp 103–127. DOI:https://doi.org/10.1016/B978-0-12-811488-9.00006-8
21. Wang X, Yang X, Chen S, Li Q, Wang W, Hou C, Gao X, Wang L, Wang S. Zinc oxide nanoparticles affect biomass accumulation and photosynthesis in arabidopsis. Front Plant Sci. 2016;6:559. https://doi.org/10.3389/fpls.2015.01243.
22. Costa MVJ, Sharma PK. Effect of copper oxide nanoparticles on growth, morphology, photosynthesis, and antioxidant response in Oryza sativa. Photosynthetica. 2016;54:110–9. https://doi.org/10.1007/s11099-015-0167-5.
23. Barhoumi L, Oukarroum A, Taher LB, Smiri LS, Abdelmelek H, Dewez D. Effects of superparamagnetic iron oxide nanoparticles on photosynthesis and growth of the aquatic plant Lemna gibba. Arch Environ Contam Toxicol. 2015;68:510–20. https://doi.org/10.1007/s00244-014-0092-9.
24. Kun Q, Tianyu S, Tao T, Shaoliang Z, Xili and Liu,. Preparation and characterization of nano-sized calcium carbonate as controlled release pesticide carrier for validamycin against Rhizoctonia solani. Microchim Acta. 2010;173:51–7. https://doi.org/10.1007/s00604-010-0523-x.
25. Boyjoo Y, Pareek VK, Liu J. Synthesis of micro and nano-sized calcium carbonate particles and their applications. J Mater Chem. 2014;2:14270–88. https://doi.org/10.1039/C4TA02070G.
26. Hua KH, Wang HC, Chung RS, Hsu JC. Calcium carbonate nanoparticles can enhance plant nutrition and insect pest tolerance. J Pestic Sci. 2015;40:208–13. https://doi.org/10.1584/jpestics.D15-025.
27. Tantawy AS, Salama YAM, Abdel-Mawgoud AMR, Ghoname AA. Comparison of chelated calcium with nano calcium on alleviation of salinity negative effects on tomato plants. Middle East J Agric Res. 2014;3:912–6.
28. Liang W, Wang M, Ai X. The role of calcium in regulating photosynthesis and related physiological indexes of cucumber seedlings under low light intensity and suboptimal temperature stress. Sci Hortic. 2009;123:34–8. https://doi.org/10.1016/j.scienta.2009.07.015.
29. Wang Q, Yang S, Wan SB, Li XG. The Significance of Calcium in Photosynthesis. Int J Mol Sci. 2019;20:1353. https://doi.org/10.3390/ijms20061353.
30. Brand JJ, Becker DW. Evidence for direct roles of calcium in photosynthesis. J Bioenerg Biomembr. 1984;16:239–49. https://doi.org/10.1007/BF00744278.
31. Qian H, Hu Y, Liu Y, Zhou M, Guo C. Electrostatic self-assembly of TiO2 nanoparticles onto carbon spheres with enhanced adsorption capability for Cr(VI). Mater Lett. 2012;68:174–7. https://doi.org/10.1016/j.matlet.2011.10.054.
32. Andersen F, Brečević L, Beuter G, Dell'Amico D, Calderazzo F, Bjerrum N, Underhill A. Infrared Spectra of Amorphous and Crystalline Calcium Carbonate. Acta Chem Scand. 1991;45:1018–24. https://doi.org/10.3891/acta.chem.scand.45-1018.
33. Gao Y, Li J, Hu Z, Shi Y. Effects of Acetochlor on Wheat Growth Characteristics and Soil Residue in Dryland. Gesunde Pflanzen. 2021;73:307–15. https://doi.org/10.1007/s10343-021-00553-7.
34. Du Z, Bramlage WJ. Modified thiobarbituric acid assay for measuring lipid oxidation in sugar-rich plant tissue extracts. Jagricfoodchem. 1992;40:1566–70. https://doi.org/10.1021/jf00021a018.
35. Wang X, Li Q, Xie JJ, Huang M, Cai J, Zhou Q, Dai TB, Jiang D. Abscisic acid and jasmonic acid are involved in drought priming-induced tolerance to drought in wheat. Crop J. 2021;9:120–32. https://doi.org/10.1016/j.cj.2020.06.002.
36. Patra HK, Kar M, Mishra D. Catalase Activity in Leaves and Cotyledons During Plant Development and Senescence1)1) Part X of the series "Studies on Leaf Senescence". Supported in part by a Grant from the Council of Scientific and Industrial Research, Government of India to D.M. Biochem Physiol Pflanz. 1978;172:385–90. https://doi.org/10.1016/S0015-3796(17)30412-2.
37. Nakano Y, Asada K. Hydrogen peroxide is scavenged by ascorbate-specific peroxidase in spinach chloroplasts. Plant Cell Physiol. 1980;22:867–80. https://doi.org/10.1093/oxfordjournals.pcp.a076232.
38. Linchenthaler HR, Wellburn AR. Determination of total carotenoids and chlorophyll a and b of leaf extracts in different solvents. Biochem Soc Trans. 1983;11:1591–2.
39. Qin WJ, Yan HY, Zou BY, Guo RZ, Ci DW, Tang ZH, Zou XX, Zhang XJ, Yu XN, Wang YF, Si T. Arbuscular mycorrhizal fungi alleviate salinity stress in peanut: Evidence from pot-grown and field experiments. Food Energy Security. 2021;10:e314. https://doi.org/10.1002/fes3.314.
40. Wang X, Zhang X, Chen J, Wang X, Cai J, Zhou Q, Dai T, Cao W, Jiang D. Parental drought-priming enhances tolerance to post-anthesis drought in offspring of wheat. Front Plant Sci. 2018;9:261. https://doi.org/10.3389/fpls.2018.00261.
41. Dong HH, Luo YL, Li WQ, W YY, Zhang QX, Chen J, Jin M, Li Y and Wang ZI,. Effects of Different Spring Nitrogen Topdressing Modes on Lodging Resistance and Lignin Accumulation of Winter Wheat. Scientia Agricultura Sinica. 2020;53:4399–414. https://doi.org/10.3864/j.issn.0578-1752.2020.21.009.
42. Cao JL, Zeng Q, Zhu JG. Responses of photosynthetic characteristics and gene expression in different wheat cultivars to elevated ozone concentration at grain filling stage. Acta Agron Sin. 2022;48:2339–50.
43. Pathak J, Ahmed H, Kumari N, Pandey A, Rajneesh and Sinha RP (2020) Role of Calcium and Potassium in Amelioration of Environmental Stress in Plants. Role of Calcium and Potassium in Amelioration of Environmental Stress in Plants. In Protective Chemical Agents in the Amelioration of Plant Abiotic Stress (eds A. Roychoudhury and D.K. Tripathi), pp 535–562. DOI: https://doi.org/10.1002/9781119552154.ch27

44. Domingues LdS, Ribeiro ND, Andriolo JL, Possobom MTDF, Zemolin AEM. Growth, grain yield and calcium, potassium and magnesium accumulation in common bean plants as related to calcium nutrition. Acta Sci Agron. 2016;38:207–17. https://doi.org/10.4025/actasciagron.v38i2.27757.
45. Chao Y-Y, Wang W-J, Liu Y-T. Effect of Calcium on the Growth of Djulis (Chenopodium formosanum Koidz.) Sprouts. Agronomy. 2021;11:82. https://doi.org/10.3390/agronomy11010082.
46. Petrochenko K, Kurovsky A, Godymchuk A, Babenko A, Yakimov Y, Gusev A. A case study of woody leaf litter vermicompost as a promising calcium fertilizer. Bulgarian J Agr Sci. 2019;25:646–53.
47. Singh SK, Chien CT, Chang IF. The Arabidopsis glutamate receptor-like gene GLR3.6 controls root development by repressing the Kip-related protein gene KRP4. J Exp Bot. 2016;67:1853–69. https://doi.org/10.1093/jxb/erv576.
48. Martínez-Fernández D, Barroso D, Komárek M. Root water transport of Helianthus annuus L. under iron oxide nanoparticle exposure. Environ Sci Pollut Res. 2016;23:1732–41. https://doi.org/10.1007/s11356-015-5423-5.
49. Wang P, Bi S, Ma L, Han W. Aluminum tolerance of two wheat cultivars (Brevor and Atlas66) in relation to their rhizosphere pH and organic acids exuded from roots. J Agric Food Chem. 2006;54:10033–9. https://doi.org/10.1021/jf0611769.
50. Etxeberria E, Gonzalez P, Baroja-Fernández E, Romero JP. Fluid phase endocytic uptake of artificial nano-spheres and fluorescent quantum dots by sycamore cultured cells. Plant Signal Behav. 2006;1:196–200. https://doi.org/10.4161/psb.1.4.3142.
51. Rico CM, Majumdar S, Duarte-Gardea M, Peralta-Videa JR, Gardea-Torresdey JL. Interaction of nanoparticles with edible plants and their possible implications in the food chain. J Agric Food Chem. 2011;59:3485–98. https://doi.org/10.1021/jf104517j.
52. Zhai G, Walters KS, Peate DW, Alvarez PJJ, Schnoor JL. Transport of gold nanoparticles through plasmodesmata and precipitation of gold ions in woody poplar. Environ Sci Technol Lett. 2014;1:146–51. https://doi.org/10.1021/ez400202b.
53. Wong MH, Misra RP, Giraldo JP, Kwak S-Y, Son Y, Landry MP, Swan JW, Blankschtein D, Strano MS. Lipid Exchange Envelope Penetration (LEEP) of nanoparticles for plant engineering: a universal localization mechanism. Nano Lett. 2016;16:1161–72. https://doi.org/10.1021/acs.nanolett.5b04467.
54. Li L, Luo Y, Li R, Zhou Q, Peijnenburg WJGM, Yin N, Yang J, Tu C, Zhang Y. Effective uptake of submicrometre plastics by crop plants via a crack-entry mode. Nature Sustainability. 2020;3:929–37. https://doi.org/10.1038/s41893-020-0567-9.
55. Khan MN, Mobin M, Abbas ZK, AlMutairi KA, Siddiqui ZH. Role of nanomaterials in plants under challenging environments. Plant Physiol Biochem. 2017;110:194–209. https://doi.org/10.1016/j.plaphy.2016.05.038.
56. Weng XH, Li H, Ren CS, Zhou YB, Zhu WX, Zhang SZ, Liu LY. Calcium Regulates Growth and Nutrient Absorption in Poplar Seedlings. Front Plant Sci. 2022. https://doi.org/10.3389/fpls.2022.887098.
57. Liang CJ, Zhang BJ. Effect of exogenous calcium on growth, nutrients uptake and plasma membrane H+-ATPase and Ca2+-ATPase activities in soybean (Glycine max) seedlings under simulated acid rain stress. Ecotoxicol Environ Saf. 2018;165:261–9. https://doi.org/10.1016/j.ecoenv.2018.09.019.
58. Soliman A, Elfeky S, Darwish E. Alleviation of salt stress on Moringa peregrina using foliar application of nanofertilizers. Journal of Horticulture and Forestry. 2015;7:36–47. https://doi.org/10.5897/JHF2014.0379.
59. Zaimenko NV, Didyk NP, Dzyuba OI, Zakrasov OV, Rositska NV and Viter AV (2014) Enhancement of Drought Resistance in Wheat and Corn by Nanoparticles of Natural Mineral Analcite. Ecologia Balkanica 6.
60. Shabbir R, Javed T, Hussain S, Ahmar S, Naz M, Zafar H, Pandey S, Chauhan J, Siddiqui MH, Pinghua C. Calcium homeostasis and potential roles to combat environmental stresses in plants. S Afr J Bot. 2022;148:683–93. https://doi.org/10.1016/j.sajb.2022.05.038.
61. Tian W, Wang C, Gao Q, Li L, Luan S. Calcium spikes, waves and oscillations in plant development and biotic interactions. Nature Plants. 2020;6:750–9. https://doi.org/10.1038/s41477-020-0667-6.
62. Dvorak P, Krasylenko Y, Zeiner A, Samaj J, Takac T. Signaling Toward Reactive Oxygen Species-Scavenging Enzymes in Plants. Front Plant Sci. 2021. https://doi.org/10.3389/fpls.2020.618835.
63. Dale S, Jerome P, Colin B, Harper JF. Calcium at the Crossroads of Signaling. Plant Cell. 2002. https://doi.org/10.1105/tpc.002899.
64. Costa A, Luoni L, Marrano CA, Hashimoto K, Koster P, Giacometti S, De Michelis MI, Kudla J, Bonza MC. Ca2+-dependent phosphoregulation of the plasma membrane Ca2+-ATPase ACA8 modulates stimulus-induced calcium signatures. J Exp Bot. 2017;68:3215–30. https://doi.org/10.1093/jxb/erx162.
65. Poddar K, Sarkar D and Sarkar A (2020) Nanoparticles on Photosynthesis of Plants: Effects and Role. In: Patra JK, Fraceto LF, Das G and Campos EVR (eds) Green Nanoparticles: Synthesis and Biomedical Applications Springer International Publishing, Cham, pp 273–287. DOI: https://doi.org/10.1007/978-3-030-39246-8_13
66. Taylor SH, Long SP. Slow induction of photosynthesis on shade to sun transitions in wheat may cost at least 21% of productivity. Philos Trans R Soc Lond B Biol Sci. 2017. https://doi.org/10.1098/rstb.2016.0543.
67. Zhang Z, Wu P, Zhang W, Yang Z, Liu H, Ahammed GJ, Cui J. Calcium is involved in exogenous NO-induced enhancement of photosynthesis in cucumber (Cucumis sativus L) seedlings under low temperature. Sci Hortic. 2020;261:108953. https://doi.org/10.1016/j.scienta.2019.108953.
68. Iida S, Kobiyama A, Ogata T, Murakami A. Differential DNA Rearrangements of Plastid Genes, psbA and psbD, in Two Species of the Dinoflagellate Alexandrium. Plant Cell Physiol. 2010;51:1869–77. https://doi.org/10.1093/pcp/pcq152.
69. Gao F, Hong F, Liu C, Zheng L, Su M, Wu X, Yang F, Wu C, Yang P. Mechanism of nano-anatase TiO2 on promoting photosynthetic carbon reaction of spinach. Biol Trace Elem Res. 2006;111:239–53. https://doi.org/10.1385/BTER:111:1:239.
70. Spreitzer RJ. Questions about the complexity of chloroplast ribulose-1,5-bisphosphate carboxylase/oxygenase. Photosynth Res. 1999;60:29–42. https://doi.org/10.1023/A:1006240202051.
71. Singh R, Parihar P, Singh S, Mishra RK, Singh VP, Prasad SM. Reactive oxygen species signaling and stomatal movement: Current updates and future perspectives. Redox Biol. 2017;11:213–8. https://doi.org/10.1016/j.redox.2016.11.006.
72. Lawson T. Guard cell photosynthesis and stomatal function. New Phytol. 2009;181:13–34. https://doi.org/10.1111/j.1469-8137.2008.02685.x.

Publisher's Note